

Saddle-node bifurcation: Appearance mechanism of pulses in the subcritical complex Ginzburg-Landau equation

O. Descalzi

Facultad de Ingeniería, Universidad de los Andes, Avenida San Carlos de Apoquindo 2200, Santiago, Chile

M. Argentina and E. Tirapegui

Departamento de Física, FCFM Universidad de Chile, Casilla 487-3, Santiago, Chile

(Received 4 February 2002; published 21 January 2003)

We study stationary, localized solutions in the complex subcritical Ginzburg-Landau equation in the region where there exists coexistence of homogeneous attractors. Using a matching approach, we report on the fact that the appearance of pulses are related to a saddle-node bifurcation. Numerical simulations are in good agreement with our theoretical predictions.

DOI: 10.1103/PhysRevE.67.015601

PACS number(s): 05.45.-a, 82.40.Bj, 89.75.Kd

Spatially extended nonequilibrium systems often show coherent or localized structures that may take the form of propagating kinks, oscillating pulses, or standing fronts, to mention a few (for a survey, see Ref. [1]). The dynamics of these localized structures may be either stationary, periodic, or chaotic. A famous example is the motion of a localized and turbulent region surrounded by laminar flows, which appears in many open flow experiments [2], such as Taylor-Couette flow with counter-rotating cylinder channel flows [3], plane Poiseuille flow [4,5]. At the onset of binary fluid convection, standing and localized waves have also been observed [6–10]. Localized oscillations in vibrating granular layer constitute another example [11,12]. More recently, experiments in electroconvection of nematic liquid crystals showed that localized structures may eventually bifurcate to chaos [13]. Hence, it appears quite important to understand what are the mechanisms of creation, or the physical features necessary, to sustain such structures. Some approaches permit to describe the existence of these entities. For example, pinning effect of local compact structures (periodic standing wave in one spatial dimensions) permit to explain the existence of such localized entities [14,15]. Another approach is the study of subcritical instabilities, where two stable states may coexist for some range of parameters, and this is the situation we consider here. We shall study the localized oscillating solutions observed in the subcritical Ginzburg-Landau equation that can be written as

$$\partial_t A = \mu A + (\beta_r + i\beta_i)|A|^2 A + (\gamma_r + i\gamma_i)|A|^4 A + \partial_{xx} A, \quad (1)$$

where $A(x,t) = r \exp i\phi$ is a complex field. Here dispersive effects have been neglected and will be taken into account elsewhere. Great efforts have been devoted to the study of this equation [16–24,26–29]. The signs of the parameters $\beta_r > 0$ and $\gamma_r < 0$ are chosen in order to guarantee that the bifurcation is subcritical and saturates to quintic order. Equation (1) admits a class of homogeneous time-periodic solutions,

$$A_{1,2} = r_{1,2} \exp[i([\beta_i r_{1,2}^2 + \gamma_i r_{1,2}^4]t + \varphi_0)], \quad (2)$$

where $r_{1,2}^2 = (-\beta_r \pm \sqrt{\beta_r^2 - 4\gamma_r \mu})/2\gamma_r$ and φ_0 is an arbitrary phase. The existence of solutions $A_{1,2}$ requires that $\mu \geq \beta_r^2/4\gamma_r$. However, inside this range only A_2 is stable against small perturbations. It is easy to see that $A_0 = 0$ is also a solution of Eq. (1), but it is stable only for $\mu < 0$. Therefore the stable solutions A_0 and A_2 coexist for $\beta_r^2/4\gamma_r \leq \mu \leq 0$. Inside this region, where the stable homogeneous solutions coexist, numerically oscillating stable pulses have been observed [25–29].

The aim of this paper is to present an explicit analytic approximation of these pulses which also exhibits in a clear way their mechanism of appearance, which is a saddle-node bifurcation. This mechanism is well known in the variational [16,17] and in the conservative limits [27], and our approximation shows that far away from these two limit cases pulses appear and disappear through a saddle-node bifurcation. Our strategy consists of calculating the pulse inside and outside the core and then to match the approximate solutions in the border of the regions, imposing there continuity of the amplitude, the phase, and the derivative of the amplitude.

The starting point is the ansatz $r = R_0(x)$, $\phi = \Omega t + \theta_0(x)$, where Ω is the oscillating frequency of the pulse, which is an unknown parameter to be determined. This ansatz has been first introduced in Ref. [26]. We assume that the tails of the pulses go to zero at infinity [$\lim_{|x| \rightarrow \infty} R_0(x) = 0$]. Replacing this ansatz in Eq. (1), we obtain the following equations:

$$0 = \mu R_0 + \beta_r R_0^3 + \gamma_r R_0^5 + R_{0,xx} - R_0 \theta_{0,x}^2, \quad (3)$$

$$\Omega R_0 = \beta_i R_0^3 + \gamma_i R_0^5 + 2R_{0,x} \theta_{0,x} + R_0 \theta_{0,xx}. \quad (4)$$

To solve Eqs. (3) and (4) we proceed to separate the pulse in two regions, namely, inside the core and outside the core of the pulse, and then we perform a matching. Inside the core we suppose that the module $R_0(x)$ admits a Taylor expansion, so that

$$R_0(x) = R_m - \epsilon x^2 + o(x^4), \quad (5)$$

where R_m is the greatest value of $R_0(x)$, and the second unknown. At leading order, the Taylor expansion of the phase gradient is determined by

$$\theta_{0x}(x) = -\alpha x + o(x^3). \quad (6)$$

We suppose that the pulse is not breaking the reflection symmetry ($x \rightarrow -x$). Replacing $R_0(x)$ and $\theta_{0x}(x)$ in Eqs. (3) and (4), we obtain

$$\begin{aligned} \epsilon &= \frac{1}{2}(\mu R_m + \beta_r R_m^3 + \gamma_r R_m^5), \\ \alpha &= \beta_i R_m^2 + \gamma_i R_m^4 - \Omega. \end{aligned} \quad (7)$$

Of course, we can include higher-order terms in Eqs. (5) and (6), but they are not necessary for the purpose of this paper.

At dominant order and outside the core of the pulse, we suppose that the phase gradient $\theta_{0x}(x)$ is determined by $\theta_{0x}(x) = p$ for $x < 0$ and $\theta_{0x}(x) = -p$ for $x > 0$. Since $R_0(x)$ goes asymptotically to zero, from Eqs. (3) and (4), we deduce

$$\Omega = 2p\sqrt{-\mu + p^2}. \quad (8)$$

We then see that Ω is related to p , and we remain finally with two unknowns: R_m and p . Solving Eq. (3) in the bulk, where the phase gradient is constant, we obtain

$$R_0(x) = \frac{2b^{1/4} \exp\{\sqrt{-\mu + p^2}(|x| + x_0)\}}{\sqrt{\left(\exp\{2\sqrt{-\mu + p^2}(|x| + x_0)\} + \frac{a}{\sqrt{b}}\right)^2 - 4}}, \quad (9)$$

where $a = -3\beta_r/2\gamma_r$ and $b = -3(-\mu + p^2)/\gamma_r$.

Once we have calculated $R_0(x)$ inside and outside the core of the pulse, we proceed to match both functions at the point $(x_*, r_c) = (-p/\alpha, R_m - \epsilon x_*)$, where r_c is the value of $R_0(x)$ at the matching point. Using $R_0(x)$ outside the core, by inverting relation (9), we get

$$u_*^2 = -\frac{a}{\sqrt{b}} + \frac{2\sqrt{b}}{r_c^2} + \frac{2}{r_c^2} \sqrt{r_c^4 - ar_c^2 + b}, \quad (10)$$

where $u_* = \exp\{-\sqrt{-\mu + p^2}(x_* - x_0)\}$. Then $x_0 = x_* + (\ln u_*/\sqrt{-\mu + p^2})$.

We now impose that the derivative $dR_0(x)/dx$ outside the core [Eq. (9)] and inside the core [Eq. (5)] should be equal at $x = x_*$. This gives a first relation between R_m and p , which reads

$$\sqrt{-\frac{\gamma_r}{3} r_c \sqrt{r_c^4 - ar_c^2 + b} + 2\epsilon x_*} = 0. \quad (11)$$

From now on we shall refer to Eq. (11) as $f(R_m, p) = 0$. We need a second relation in order to be able to fix the free parameters $\{R_m, p\}$ of the ansatz, and it can be obtained (following Ref. [26]) by multiplying Eq. (4) by $R_0(x)$ and integrating in the whole domain. This gives

$$\Omega - \beta_i \frac{\int_{-\infty}^0 R_0^4 dx}{\int_{-\infty}^0 R_0^2 dx} - \gamma_i \frac{\int_{-\infty}^0 R_0^6 dx}{\int_{-\infty}^0 R_0^2 dx} = 0. \quad (12)$$

The integrals in Eq. (12) can be evaluated, and one gets

$$\begin{aligned} \int_{-\infty}^0 R_0^2 dx &= \frac{\sqrt{b}}{2\sqrt{-\mu + p^2}} \ln \left| \frac{a + \sqrt{b}(u_*^2 + 2)}{a + \sqrt{b}(u_*^2 - 2)} \right| - R_m^2 x_* \\ &\quad + \frac{2}{3} R_m \epsilon x_*^3. \end{aligned} \quad (13)$$

$$\begin{aligned} \int_{-\infty}^0 R_0^4 dx &= -\frac{(a^2 - 4b)b + ab\sqrt{b}u_*^2}{\sqrt{-\mu + p^2}[-4b + (a + \sqrt{b}u_*^2)^2]} \\ &\quad + \frac{a\sqrt{b} \ln \left| \frac{a + \sqrt{b}(u_*^2 + 2)}{a + \sqrt{b}(u_*^2 - 2)} \right|}{4\sqrt{-\mu + p^2}} - R_m^4 x_* + \frac{4}{3} R_m^3 \epsilon x_*^3. \end{aligned} \quad (14)$$

$$\begin{aligned} \int_{-\infty}^0 R_0^6 dx &= \frac{\sqrt{b}}{16\sqrt{-\mu + p^2}[-4b + (a + \sqrt{b}u_*^2)^2]^2} \\ &\quad \times \left(-12a\sqrt{b}(a^2 - 4b)^2 - 4bu_*^2(a^2 - 4b)(9a^2 + 4b) - 12a(3a^2 - 4b)b^{3/2}u_*^4 + 4b^2(-3a^2 + 4b)u_*^6 + (3a^2 - 4b)[-4b + (a + \sqrt{b}u_*^2)^2]^2 \right. \\ &\quad \left. \times \ln \left| \frac{a + \sqrt{b}(u_*^2 + 2)}{a + \sqrt{b}(u_*^2 - 2)} \right| \right) - R_m^6 x_* + 2R_m^5 \epsilon x_*^3. \end{aligned} \quad (15)$$

The above integrals together with the value of Ω given by relations (8) and (12) enable us to obtain the second relation, which from now on will be referred as $g(R_m, p) = 0$. The matching is accomplished by computing $\{R_m, p\}$, such that $f = g = 0$.

With these schemes, two pulses are found in a finite region for negative μ , and one pulse for positive μ . We draw the curves $f(R_m, p) = 0$ (continuous line) and $g(R_m, p) = 0$ (dashed line), considering $\mu = -0.486$ in Fig. 1(a). It is seen that the curves intersect twice, implying the existence of two pulses. By further decreasing μ , the curves do not cross at any point, suggesting that the pulses do not exist anymore [see Fig. 1(b)]. At $\mu = \mu_c = -0.489$, the two solutions disappear by coalescence. This disappearance is therefore associated to a saddle-node bifurcation occurring in the functional space. Hence, after the bifurcation, $\mu > \mu_c$, one solution must be stable and the other one unstable. In such a case, the spectrum of the linearized operator at the unstable pulse has a unique positive eigenvalue. Hence the codimension-1 stable manifold of the unstable pulse must act

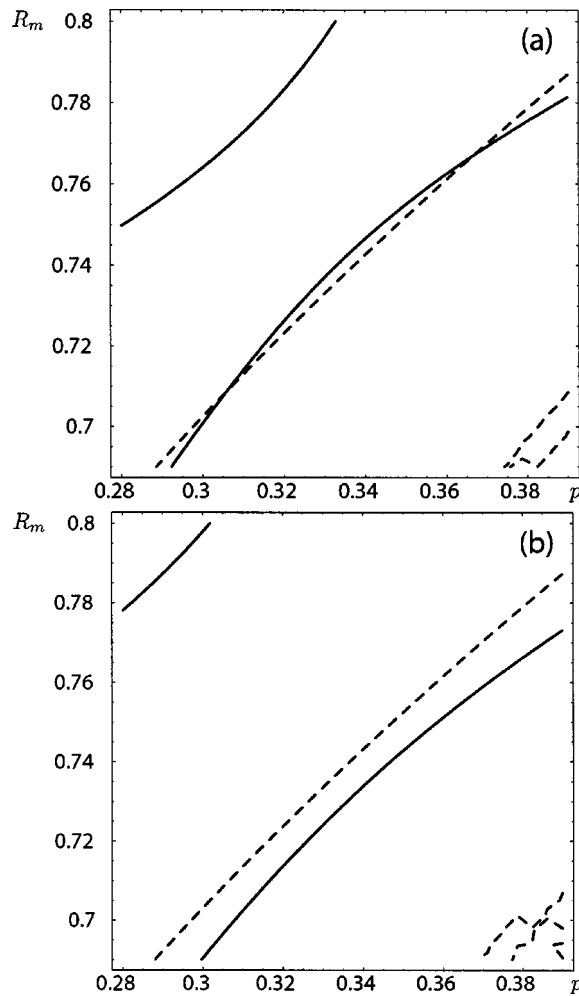


FIG. 1. (a) For $\mu = -0.486 > \mu_c$ the curves cut at two points, giving origin to pulses with $(R_m = 0.708, p = 0.305)$ and $(R_m = 0.767, p = 0.366)$. (b) For $\mu = -0.5 < \mu_c$, the curves do not cut at any point: there are no pulses. Values of the parameters are $\beta_r = 3$, $\beta_i = 1$, $\gamma_r = -2.75$, and $\gamma_i = 1$. The value of μ_c is -0.489 .

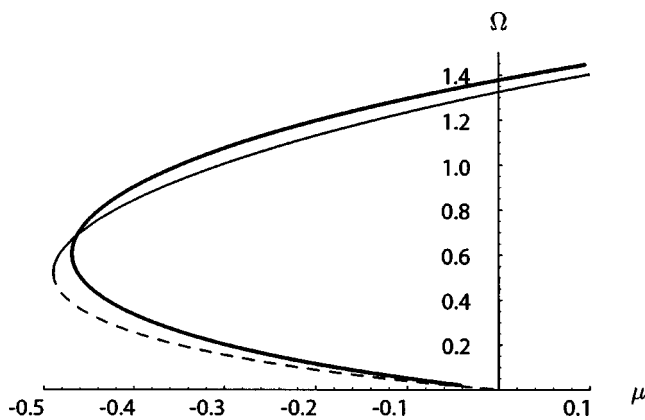


FIG. 2. Bifurcation diagram for pulses. The thin continuous line corresponds to stable pulses and the thin dashed line to unstable pulses. These two branches are computed from the analytical approximation. The thick continuous line is computed with the bifurcation software AUTO 2000. The values of the parameters are the same as in Fig. 1.

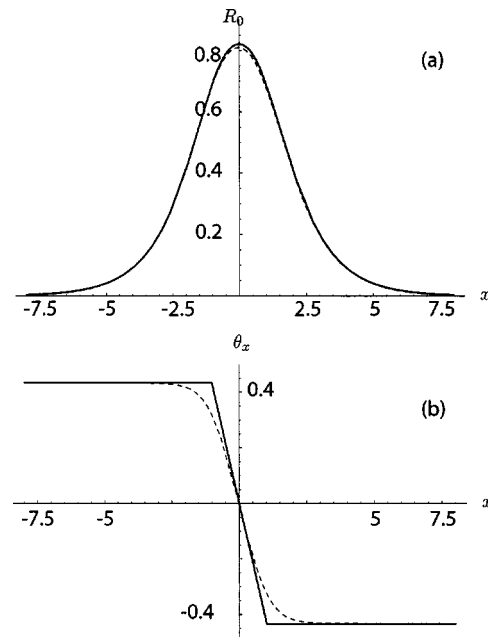


FIG. 3. (a) Shape of the stable pulse predicted by the analytical approach (continuous line) and by numerics (dashed line). (b) The gradient of the phase.

as a separatrix in functional space determining the nucleation barrier that permits the creation of the stable pulse from the homogeneous state. To see explicitly the character of the saddle-node bifurcation, we calculate Ω as a function of μ (see Fig. 2) using the bifurcation software AUTO 2000 [30]. We obtain the two expected branches, and we compare them

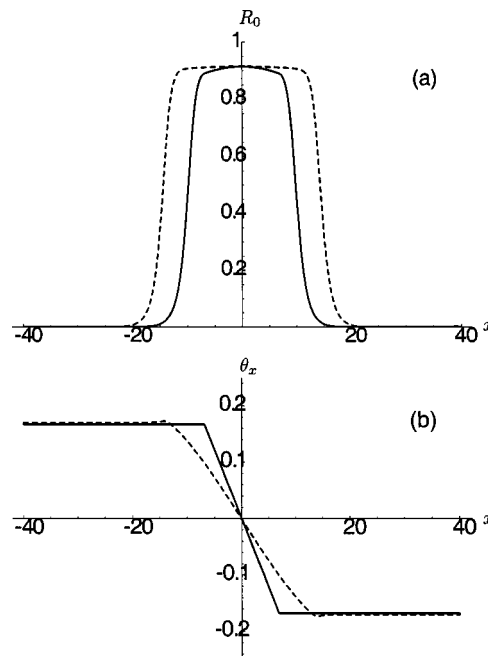


FIG. 4. (a) Module of the stable pulse close to the Maxwell point predicted by the analytical approach (continuous line) and by a numerical simulation (dashed line). Parameter values are $\mu - \mu_M = 0.0286$, $\beta_r = 3$, $\beta_i = 0.343$, $\gamma_r = -2.75$, and $\gamma_i = 0$. (b) The gradient of the phase.

with the analytical approximation. One of them corresponds to the stable pulses and the other one to the unstable pulses.

The lower branch appears at $\mu=0$, and this is understood as a bifurcation of the homogeneous state A_0 . Since this latter is subcritical, this means that the lower branch represents unstable solutions. By further decreasing the parameter μ , the lower branch folds into the upper one: this is the saddle-node bifurcation reported above. Direct numerical simulation show that points in the upper branch correspond, as expected, to stable pulses.

The analytical prediction is also checked with a numerical integration of Eq. (1): it results that for $\mu < -0.468$ there are no stable pulses. This result agrees within 5% with our approach. To compare the shape of the pulses, we consider the particular value of $\mu = -0.46$ and the parameters mentioned above. Our approximation predicts two pulses after the curves $f(R_m, p) = 0$ and $g(R_m, p) = 0$ cut in two points, namely $(p = 0.250, R_m = 0.643)$ and $(p = 0.434, R_m = 0.821)$.

In Fig. 3 we show the shape and the phase gradient of the pulse obtained with our analytical approach (continuous line) and with our numerical simulation (dashed line). The values of R_m , the asymptotical value of the phase gradient, and the sizes of the stable pulses agree within 1% with our approximation.

One interesting limit to be studied is the variational limit. As it is known from Ref. [16] in this limit, pulses exist inside a finite interval limited by two saddle-node bifurcation curves. This interval converges to zero as we approach the Maxwell point ($\mu \rightarrow \mu_M = 3\beta_r^2/16\gamma_r; \beta_i \rightarrow 0; \gamma_i \rightarrow 0$). Our

method generates pulses with a similar shape to those obtained directly from the numerical simulation. Figure 4 shows the module and the phase gradient of one stable pulse close to the Maxwell point. We can see that the values of R_m and the asymptotical value of the phase gradient of our analytical approximation are very close to the exact values obtained from the numerical simulation. Moreover, we obtain from our method that the width of the pulses diverges as $\mu \rightarrow \mu_M$.

In conclusion, using a simple method we have constructed approximately pulses in the complex subcritical Ginzburg-Landau equation with nondispersive terms. However, this restriction may be overcome [31], and the conservative limit can then be approached using the same procedure. The approximation scheme presented here is valid through the whole intermediate range of parameters between the variational and the conservative limit, and remains valid in both limits as we have discussed.

E.T. and O.D. wish to thank the Fondo de Ayuda a la Investigación of the Universidad de los Andes (Project No. ICIV-001-02) and the FONDECYT (Project No. 1020374). M.A. acknowledges support from the FONDECYT (Project No. 3000017). We would like to thank Professor M. G. Clerc (Universidad de Chile) and Professor H. R. Brand (Universität Bayreuth, Germany) for many useful discussions. The numerical simulation has been performed using the software developed in the Institut Non-linéaire de Nice, France. We are indebted to Professor P. Couillet (Nice) for allowing us to use this software.

-
- [1] M.C. Cross and P.C. Hohenberg, *Rev. Mod. Phys.* **65**, 851 (1993), and references therein.
- [2] D. J. Tritton, *Physical Fluid Dynamics* (Van Nostrand Reinhold, New York, 1977), Chap. 19.
- [3] J.J. Hegseth, C.D. Andereck, F. Hayot, and Y. Pomeau, *Phys. Rev. Lett.* **62**, 257 (1989).
- [4] See M.J. Landman, *Stud. Appl. Math.* **76**, 187 (1987), and references therein.
- [5] R.J. Deissler, *J. Stat. Phys.* **54**, 1459 (1989).
- [6] J.J. Niemela, G. Ahlers, and D.S. Cannell, *Phys. Rev. Lett.* **64**, 1365 (1990).
- [7] E. Moses, J. Fineberg, and V. Steinberg, *Phys. Rev. A* **35**, 2757 (1987).
- [8] P. Kolodner, D. Bensimon, and C.M. Surko, *Phys. Rev. Lett.* **60**, 1723 (1988).
- [9] R. Heinrichs, G. Ahlers, and D.S. Cannell, *Phys. Rev. A* **35**, 2761 (1987).
- [10] P. Kolodner, C.M. Surko, A. Passner, and H. L. Williams, *Phys. Rev. A* **36**, 2499 (1987).
- [11] P. Umbanhowar, F. Melo, H.L. Swinney, *Nature (London)* **382**, 793 (1996).
- [12] I.S. Aranson, L.S. Tsimring, *Physica A* **249**, 103 (1998).
- [13] L. Pastur, M. Henriot, and R. Ribotta, *Phys. Rev. Lett.* **86**, 228 (2001).
- [14] P. Couillet, C. Riera, and C. Tresser, *Phys. Rev. Lett.* **84**, 3069 (2000).
- [15] Y. Pomeau, *Physica (Amsterdam)* **23**, 3 (1986).
- [16] V. Hakim and Y. Pomeau, *Eur. J. Mech. B/Fluids* **10**, 137 (1991).
- [17] B.A. Malomed and A.A. Nepomnyashchy, *Phys. Rev. A* **42**, 6009 (1990).
- [18] V.V. Afanasjev, N. Akhmediev, and J.M. Soto-Crespo, *Phys. Rev. E* **53**, 1931 (1996).
- [19] J.M. Soto-Crespo, N. Akhmediev, V.V. Afanasjev, and S. Wabnitz, *Phys. Rev. E* **55**, 4783 (1997).
- [20] N. Akhmediev, V.V. Afanasjev, and J.M. Soto-Crespo, *Phys. Rev. E* **53**, 1190 (1996).
- [21] R.J. Deissler and H.R. Brand, *Phys. Rev. Lett.* **72**, 478 (1994).
- [22] R.J. Deissler and H.R. Brand, *Phys. Rev. E* **51**, R852 (1995).
- [23] R.J. Deissler and H.R. Brand, *Phys. Lett. A* **146**, 252 (1990).
- [24] P. Marcq, H. Chaté, and R. Conte, *Physica D* **73**, 305 (1994).
- [25] This was observed in the study of Eq. (1) as a model of saddle-node bifurcation in extended medium; M.E. Brachet, P. Couillet, and S. Fauve, *Europhys. Lett.* **4**, 1017 (1987).
- [26] O. Thual and S. Fauve, *J. Phys. France* **49**, 1829 (1988).
- [27] S. Fauve and O. Thual, *Phys. Rev. Lett.* **64**, 282 (1990).
- [28] W. van Saarloos and P.C. Hohenberg, *Phys. Rev. Lett.* **64**, 749 (1990).
- [29] W. van Saarloos and P.C. Hohenberg, *Physica D* **56**, 303 (1992).
- [30] E.J. Doedel, H.B. Keller, and J.P. Kernévez, *Int. J. Bifurcation Chaos Appl. Sci. Eng.* **1**, 3 (1991); **1**, 4 (1991).
- [31] O. Descalzi, M. Argentina, and E. Tirapegui, *Int. J. Bifurcation Chaos* (to be published).